

Environmental Science Nano

Accepted Manuscript



This is an *Accepted Manuscript*, which has been through the Royal Society of Chemistry peer review process and has been accepted for publication.

Accepted Manuscripts are published online shortly after acceptance, before technical editing, formatting and proof reading. Using this free service, authors can make their results available to the community, in citable form, before we publish the edited article. We will replace this *Accepted Manuscript* with the edited and formatted *Advance Article* as soon as it is available.

You can find more information about *Accepted Manuscripts* in the [Information for Authors](#).

Please note that technical editing may introduce minor changes to the text and/or graphics, which may alter content. The journal's standard [Terms & Conditions](#) and the [Ethical guidelines](#) still apply. In no event shall the Royal Society of Chemistry be held responsible for any errors or omissions in this *Accepted Manuscript* or any consequences arising from the use of any information it contains.

Nano Impact: Detection and characterization of engineered nanomaterials in the environment requires sophisticated analytical techniques capable of analysis across a wide working range of concentrations and amidst a high background of naturally occurring nanoparticles. Single particle ICP-MS has been suitable technique for environmental ENP analysis, but has been ineffective at high particle number concentrations and amidst high dissolved analyte backgrounds. By utilizing microsecond dwell times, particle resolution is greatly improved, increasing the working range of this technique, while also significantly reducing signal generated from dissolved analyte. In addition, the utilization of these fast dwell times allows for the simultaneous detection of multiple elements within a single particle, opening the door for a possible means of differentiating engineered and naturally occurring nanomaterials.

ARTICLE

Improvements in the detection and characterization of engineered nanoparticles using spICP-MS with microsecond dwell times

Cite this: DOI: 10.1039/x0xx00000x

Received 00th January 2012,
Accepted 00th January 2012

DOI: 10.1039/x0xx00000x

www.rsc.org/

M. D. Montaña^a, H. R. Badiei^b, S. Bazargan^b, and J. F. Ranville^a

The imminent release of engineered nanomaterials (ENPs) into the environment has raised several questions regarding their fate, transport, and toxicity. However, their small size, expected low concentrations (ng L^{-1}), and the high environmental background of naturally occurring nanomaterials make detection and characterization difficult. In recent years, single particle ICP-MS (spICP-MS) has been developed as a promising technique to detect and characterize engineered nanoparticles in biological and environmental matrices. Improvements in the spICP-MS technique were made in this study by employing 100 microsecond dwell times. Commercially available hardware and software were developed to fully capture multiple data points over the fast transient ($\sim 500 \mu\text{s}$) nanoparticle events, which provides accurate particle sizing and counting. Reducing the background signal facilitated the characterization of Ag NPs even in the presence of ten-fold higher Ag^+ concentration. By improving the time resolution between particle events, the upper limit of the dynamic range of Ag NP concentration was increased to several $\mu\text{g L}^{-1}$. These short dwell times also provide detection of two elements in the same nanoparticle, opening the door for possible environmental applications with the prospect of obtaining particle-by-particle elemental compositions. These improvements help further establish spICP-MS as a leading analytical technique for the detection and characterization of metal-containing ENPs, and introduces new possibilities for differentiating engineered nanomaterials from their naturally occurring analogues.

Introduction

The past two decades have witnessed an exponential growth in the use of engineered nanomaterials in commercial products.¹ The novel properties that nanotechnology exhibits have proven to be worthwhile investments scientifically and economically.² With the rapid pace of manufacturing and incorporation into everyday products, release of ENPs into the environment is likely inevitable.³⁻⁶ However, the environmental and ecological risk associated with these materials is still not well understood.^{7, 8} Uncertainty regarding how many nanomaterial-containing products are in the commercial market and the minimal information on release rates from products, severely limits application of materials flow analysis in making accurate predictions of environmental concentrations.^{6, 9-13} Despite these uncertainties, risk assessment of ENPs have relied heavily on these modeling approaches mainly because of the lack of analytical methods to quantify environmental concentrations of

ENPs. In terms of analytical limitations, ENPs are expected to enter into systems containing naturally occurring nanomaterials at concentrations several orders of magnitude above the expected concentrations of the ENPs (low ng L^{-1}) and most analytical methods are not selective to ENPs only.^{9, 14} Developing techniques and methods to overcome these analytical challenges has become a priority.^{15, 16}

Single-particle ICP-MS (spICP-MS) harnesses the specificity and sensitivity of ICP-MS to detect and characterize ENPs at low-ppt concentrations.^{17, 18} Initially developed for aerosol particle analysis, spICP-MS has evolved for application to aqueous and complex matrices.¹⁹⁻²⁴ Utilizing time-resolved analysis with short dwell times, a discrete pulse of intensity originating from particle vaporization and ionization can be detected and the signal generated by the ions can be correlated to particle mass. Assuming an appropriate particle geometry (*i.e.* spherical), particle diameter can be calculated utilizing

transport efficiency determined from a standard Au NP and instrument calibration with dissolved analyte standards.^{25, 26} This technique has recently been used for metallic (gold and silver) and metal oxide (TiO₂, CeO₂) nanoparticles, carbon nanotubes, and silver nanowires in matrices ranging from animal tissues, natural and processed waters, and macroinvertebrates.²⁶⁻³³ Despite its utility, specifically for environmentally relevant samples, spICP-MS has several analytical obstacles that limit its applicability.^{25, 34}

In previous literature reports, the most commonly used dwell time has been 10 milliseconds. A number of studies suggest that under most of the commonly applied ICP-MS conditions the ion cloud generated by the particle spans only a few hundred microseconds.³⁵⁻³⁸ Consequently, 10 millisecond dwell time windows are simply too large, allowing for the possibility of several nanoparticle events to occur within this time span and therefore requiring sample dilution, which may alter the representativeness of the sample and produce low counting statistics.³⁶ The low counting statistics can be somewhat alleviated by increasing the analysis time, but this limits the use of spICPMS as a high throughput technique and also results in large data sets that must contain >90% background readings. Some investigators have attempted to improve the spICP-MS method by using dwell times on the order of 3-5 milliseconds. While reducing the chance of coincidence it introduces the problem of peak splitting, whereby the particle event is divided between two dwell times.³⁵ This necessitates recombination of split peaks and to date this has only been achieved by a laborious manual process of scanning a dataset for these events, with some researchers describing in-house spreadsheet data processing. Consequently most investigators have argued for analysis of dilute solutions utilizing dwell times > 5 millisecond or so.³⁵

A very different approach reduces the dwell times to time-scales shorter than the duration of the nanoparticle event. In contrast to millisecond spICP-MS, which relates a single point of intensity above the background to particle mass, microsecond spICP-MS produces a distribution of pulse intensities that correspond to partial sections of the ion cloud reaching the detector. In this case, multiple readings must be combined to reconstruct the particle pulse and thus obtain mass and particle number data. Previous reports have accomplished this feat through the use of sophisticated electronics and/or instrumentation that may not be widely available for most research institutions.^{36, 39} Olesik et al. demonstrated the capability of microsecond data acquisitions by amplifying the analog output from a discrete dynode detector and converting the signal to a voltage which could then be measured by a digital oscilloscope at a rate of 100,000 Hz.³⁶ Borovinskaya et al. developed a prototype time-of-flight ICP-MS for the analysis of short transient signals (~33 μs) which could also monitor multiple isotopes/elements.⁴⁰ In this paper we present a microsecond spICP-MS methodology using a standard quadrupole ICP-MS and recently developed commercial software to facilitate microsecond spICP-MS. Furthermore we highlight its advantages for reducing particle coincidence, reducing background interference from dissolved ions, and the detection of multiple elements or isotopes in single particles. With this latter capability and some knowledge of naturally occurring elemental ratios in mineral nanoparticles, it may be possible to use this technique for detecting ENPs amidst a high background of naturally occurring particles.

Results and Discussion

Improvements in Particle Resolution

With conventional millisecond dwell times, spICP-MS analyses have been relegated to using relatively low particle number concentrations (i.e. < 5x10⁶ particles L⁻¹ for a 100nm Au particle at 10 ms dwell times). These dilute concentrations are required to avoid coincidence, a phenomena that arises from two or more nanoparticles being detected within the same dwell time, effectively giving the appearance of a larger particle at a lower particle number concentration.^{18,41} It has generally been suggested that when using 10 millisecond dwell times, concentrations that result in a maximum of 5-10% of the total readings containing a particle will avoid coincidence.^{25, 34}

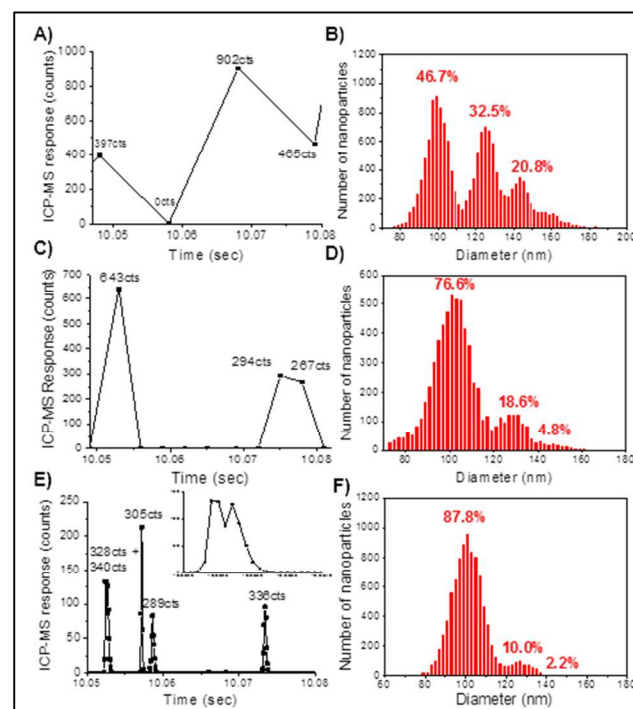


Fig. 1. Comparison of a 2 ppb solution of 100 nm gold nanoparticles sizes at 10 ms, 3 ms, and 0.1 ms. (A) Raw counts at 10 ms dwell time. (B) Particle size histogram at 10 ms. (C) Raw counts of the gold nanoparticles at 3 ms dwell times. (D) Particle size histogram of 3 ms dwell time analysis. (E) Raw counts of the gold nanoparticles at 0.1 ms dwell times (inset: magnification of first peak showing particle resolution). (F) Particle size histogram at 0.1 ms dwell times.

To demonstrate the effect of dwell time on coincidence, a series of 100 nm gold nanoparticle solutions were created at five concentrations ranging from 50 ppt to 10 ppb by mass. Figure 1 shows selected data from the analysis of a 2 ppb 100 nm gold nanoparticle solution. Figure 1A, 1C, and 1E illustrates the effect of dwell time on the raw counts of the nanoparticle. In figure 1A, at 10 ms dwell times, one background and three particle events are observed. Analysis of the 50 ppt sample at 10 msec dwell time showed a single particle registers as about 400 counts (SI) Thus it is evident that the reading at 902 counts represents multiple particles being detected within the dwell time window. Decreasing the dwell time to 3 millisecond shows greater resolution between particle events (figure 1B), as evidenced by a greater abundance of background counts

between the peaks. However there are still some data points that represent a multiple particle detection event (643 counts). Upon reducing the dwell time to 0.1 ms (100 μ s), particle resolution can be greatly enhanced to the point of defining the particle pulses (figure 1E). At 100 μ s dwell times, the nanoparticle response is parsed into bins of signal intensity as determined by the dwell time window. This allows for small changes in the number of ions present across the ion cloud to be detected. Thus even partial coincidence of particle events might be discernable if peak deconvolution methods are introduced into the signal processing. This is apparent in the first peak in figure 1E (inset in figure 1E), which shows two peaks occurring within 100 μ s of each other.

The effect of reducing dwell time on improving particle sizing is further demonstrated in figures 1B, 1D, and 1F. The percentages shown above each peak is a representation of the contribution of that peak toward the overall number of particles counted. The first peak represents the number of single 100 nm nanoparticles detected, where each subsequent peak is a result of 2 or more particles being detected simultaneously. Coincidence results in a large number of particle readings being over-sized, shifting the particle size distribution to larger diameters, which is most clearly seen at 10 millisecond dwell time (Figure 1B). At 3ms (figure 1D), the coincidence is greatly reduced, but diameters representing two particles still account for nearly 20 percent of the overall readings. At 100 μ s dwell times (figure 1E), the coincidence peak has been reduced to only 10% of the total particle readings, and is most likely an artifact of current data processing methods being unable to quantitatively resolve the two peaks, rather than the actual readings of two nanoparticles reaching the detector simultaneously. As previously mentioned, further development of peak deconvolution methods may allow coincidence to be nearly completely eliminated over the concentration ranges for which the technique would be applied.

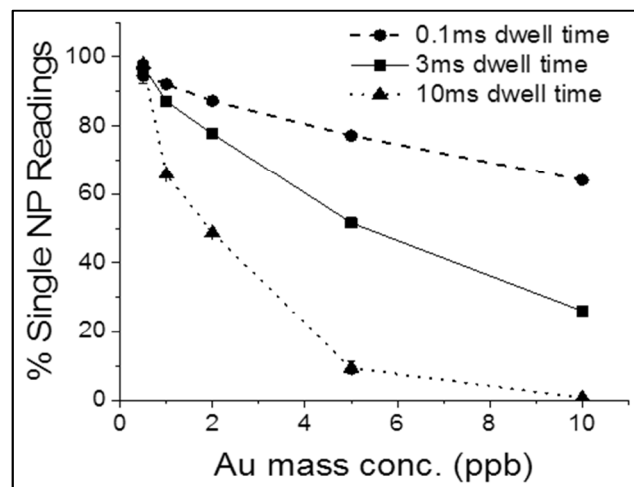


Fig. 2. Percentage of single nanoparticle readings with increasing mass (particle number) concentrations.

The need to reduce coincidence in spICP-MS is evidenced in figure 2, which demonstrates the single nanoparticle readings as a percentage of the overall particle readings (excluding background counts) as a function of mass concentration for 100 nm gold nanoparticles (error bars represent the standard deviation of triplicate measurements). At the conventional 10ms dwell time, the ability to resolve single nanoparticle

readings quickly diminishes at higher mass (particle number) concentrations. Despite being a monodisperse solution, the data collected at these millisecond dwell times would misrepresent the samples as a collection of aggregates or particles with diameters larger than 100 nm. Furthermore the measured particle number concentration will be underestimated at higher concentrations. The reduction in dwell time allows for better particle resolution, and a more accurate determination of the size distribution of the particle population even at concentrations as high as 10 μ g Au L⁻¹. This ability to improve the resolution of spICP-MS readings enhances the working range of the technique, expanding its applicability to a greater range of samples.

Reduction of dissolved analyte signal

Many samples, particularly ones obtained from the environment, contain a variety of dissolved constituents of both inorganic and organic nature. In some cases these dissolved species may be of the same elemental composition as the nanoparticle. A common method of assessing elemental concentration in aqueous samples involves the acidification of the sample to ensure the metallic constituents are equally dispersed throughout the sample and performing an element-specific analytical technique. This technique however eliminates the particulate fraction of the sample, requiring additional complementary methods (filtration, field-flow fractionation, hydrodynamic chromatography) to determine the existence of nanoparticles in the sample. By quantifying the background signal and the signal from particle pulses, spICP-MS has the unique ability to differentiate between nanoparticulate and dissolved fractions of the sample without any additional sample preparation³⁰. In practice, the cut-off between background counts and counts arising from a nanoparticle events is done through an iterative calculation where an average of the entire dataset is calculated and added to three times its standard deviation. Events above this threshold are removed from the dataset and the calculation repeated until a convergent value is reached. This value is then determined to be the cut-off between nanomaterial readings and background counts. With millisecond spICP-MS, only low concentrations (ppt) of dissolved analyte can be overcome, as under these conditions the signal generated from a nanoparticle is sufficiently large when compared to the signal from the dissolved ions. In these cases the quantification of the nanoparticle peak intensity is only a matter of subtracting the background intensity from the total intensity to generate the net intensity of the nanoparticle.²⁵

However, if dissolved concentrations reach a certain point, the signal of small nanoparticles will be lost in the noise of the background signal. This results from all ions of particular isotope being analyzed within a given dwell time, indiscriminate of particle or dissolved ion origin. An elevated background occurs where the average signal intensity of the baseline correlates to the concentration of dissolved background analyte. However, the signal generated by the particle remains the same and is a function of the mass of the analyte in the particle. As a result, once dissolved concentration are high enough, they can mask the signal of the particle, preventing differentiation between particle and background intensities.

By reducing the dwell time window, the numbers of background ions that generate a response are reduced relative to

the number of nanoparticle ions that generate a signal. This effect is seen in figure 3, where the raw signal is shown for a solution of 50ppt 60nm silver nanoparticles with a dissolved background of 500ppt dissolved silver. At 10ms, the readings generated by background and nanoparticle ions are indistinguishable. As the dwell time is decreased from 10 to 0.1 millisecond the background is reduced by a factor of 100 whereas the signal from the nanoparticle is only split between 2-3 readings. Thus the relative proportion of nanoparticle ions versus dissolved ions generating a signal increases such that the particle signal can be observed. The inset in figure 3 demonstrates that a 60 nm nanoparticle can be resolved from a background of 500 ppt Ag^+ at 100 μs dwell time observations.

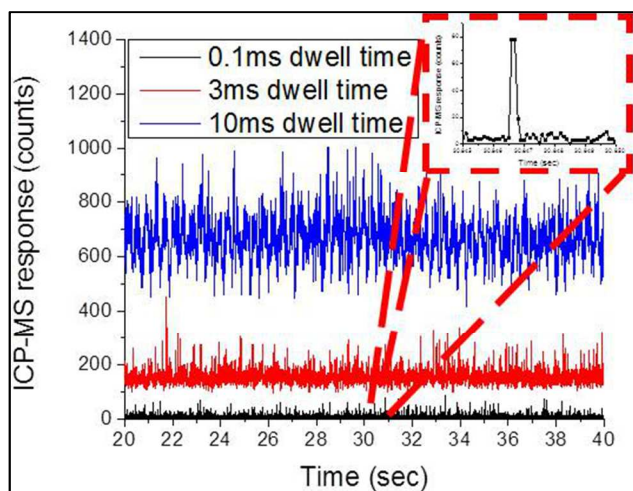


Fig. 3. Raw counts of 50 ppt 60 nm silver nanoparticles with a background of 500 ppt dissolved silver (inset: of 0.1 ms data showing particle readings above background).

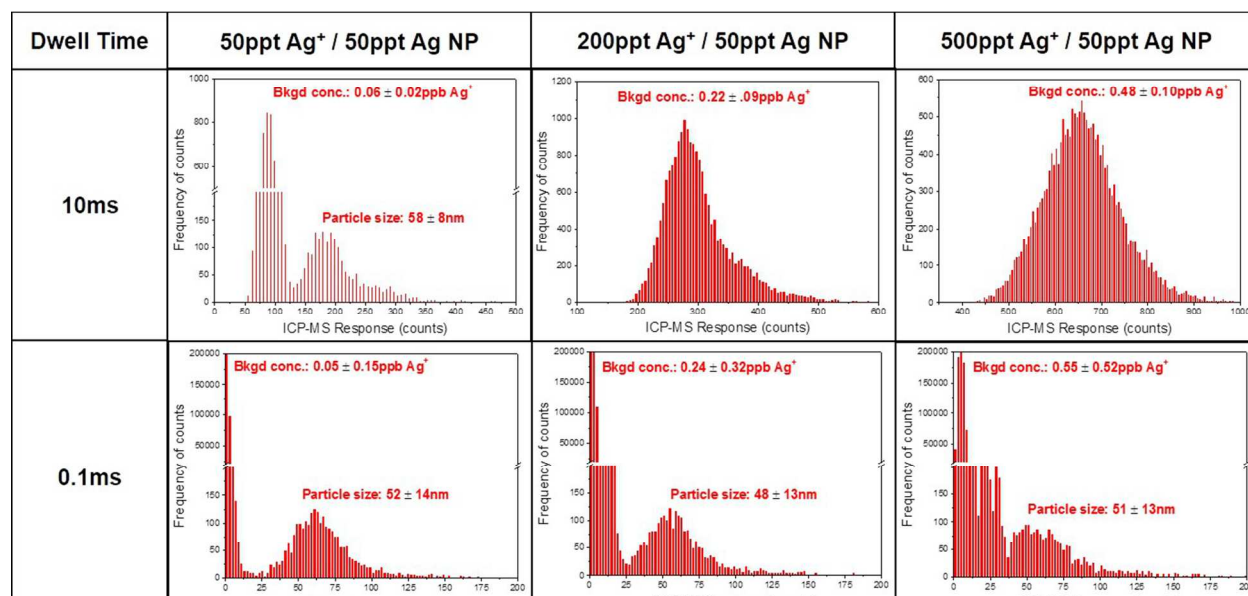
The ability of microsecond spICP-MS to improve the signal-to-noise ratio is further demonstrated in figure 4. Here a range of dissolved silver concentrations were added to a constant concentration of 50 ppt 60nm citrate-capped silver nanoparticles. In a typical distribution of count intensities, a

large initial peak of background/dissolved counts are present followed by a significantly smaller peak representing the counts generated from nanoparticles. As shown with conventional 10 ms data, the resolution between these two peaks decreases rapidly at increasing concentrations of dissolved analyte to a point where dissolved background and nanoparticle counts are indistinguishable. At 100 μs dwell times however, the resolution between the nanoparticle signal and the dissolved background signals are preserved even at dissolved analyte concentrations 10x higher than that of the nanoparticle mass concentration. This improved ability to detect and characterize nanoparticles amidst high backgrounds of dissolved analyte (*i.e.* where dissolved ion concentrations are ten times higher than particle mass concentrations) may prove essential for the analysis of ENPs *in situ*, where environmental concentrations of dissolved species are variable.

Dual-element spICP-MS

In conventional millisecond spICP-MS analyses, the analysis of a single element would encompass the entirety of the nanoparticle reading. Yet, as the nanoparticle is parsed into separate intensities in microsecond analysis, the intensities of two separate elements within a single particle can be compared and analyzed. This ability allows for isotopic and elemental ratios to be determined within a single particle if sufficient mass of the respective isotopes are present. This analysis requires that both the read and settling times are on the order of 100 microseconds or less.

This ability to perform detection of multiple isotopes at microsecond dwell times had been previously reported using a prototype time-of-flight ICP-MS.⁴² The software reported in this study allows for dual-element detection using an unmodified quadrupole ICP-MS, without the need for any additional ion separation apparatus. Though the ability to detect the full concentration of ions for a particular isotope may be lost, the ability to achieve elemental ratios could be achieved on a particle-by-particle basis.



4 | Fig. 4. Frequency distribution of raw counts for 50 ppt 60 nm silver nanoparticles with increasing concentrations of dissolved silver. Dissolved background concentrations and particle size are included as an average and standard deviation of triplicate measurements

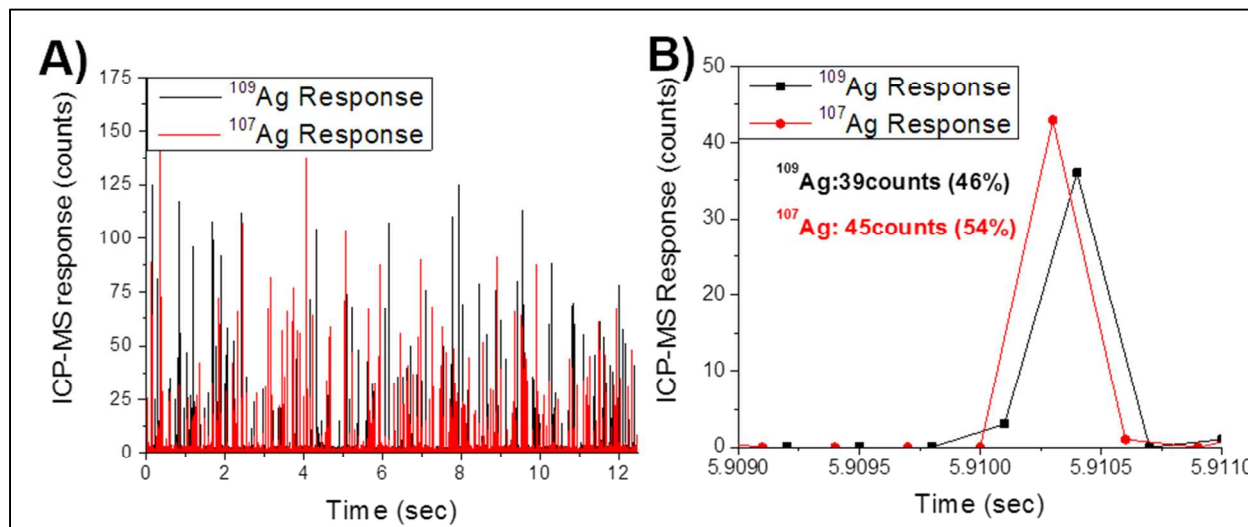


Fig. 5. Multi-element spICP-MS analysis of silver nanoparticles for ^{107}Ag and ^{109}Ag isotopes. (A) Raw counts of silver isotope data. (B) A single peak enhanced to show temporal proximity of one isotope to the other.

Figure 5 shows the analysis of a 1 ppb solution of 60 nm silver nanoparticles. As the two isotopes of silver (^{107}Ag and ^{109}Ag) occur in nearly equal ratios, it was expected that the counts generated from both isotopes would not only be detected, but in approximately equal intensities. For the data shown in figure 5, the percent abundances in the single particle shown are 46% (^{109}Ag) and 54% (^{107}Ag). An averaging of the intensities over the entire data set ($n = 125000$) gives a ratio of ^{107}Ag : 80609 counts (50.7%) and ^{109}Ag : 78245 counts (49.2%) respectively. This is very similar to the natural abundance of silver ^{107}Ag : 51.35% and ^{109}Ag : 48.65%⁴³. The ability to determine the isotopic ratio within a given nanoparticle sample adds another dimension to spICP-MS analysis that can be exploited for stable isotope analysis.

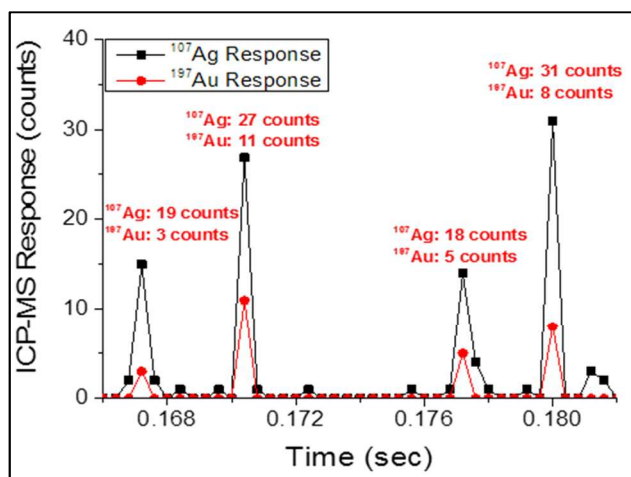


Fig. 6. Multi-element spICP-MS analysis of 30nm gold core, 30nm silver shell nanoparticle.

Perhaps more importantly than the ability to detect different isotopes of the same element, figure 6 demonstrates the capability of microsecond spICP-MS to simultaneously detect two different elements within the same particle. Here a 30 nm gold core with a 15 nm silver shell (60 nm nanometer diameter in total) was analyzed using microsecond spICP-MS. Using this technique, the two elements (^{197}Au and ^{107}Ag) were detected

within each individual particle. As expected, the silver signal was much larger as it comprises the outer shell, requiring a greater mass of silver for each subsequent layer of particle diameter. The ratio of silver to gold count intensities was consistent in dual element analysis such as in figure 5 (^{107}Ag : 255 (77.7%) and ^{197}Au : 73 counts (22.3%); $n=62$) and by single particle analysis performed individually on both elements (^{107}Ag : 880,763 (71.2%) and ^{197}Au : 356,047 counts (28.8%); $n=60,000$). The structure and composition of these Au/Ag core-shell nanoparticle was further confirmed with FFF-ICP-MS and transmission electron microscopy with energy dispersive x-ray analysis (SI figures 2-4).

The implications of detecting isotopic and elemental ratios in a single particle are significant. Of the several obstacles present in the detection and characterization of nanoparticles in the environment, the most challenging is quantification of engineered nanomaterials in the presence of significantly more ubiquitous, naturally-occurring nanomaterials. In the past, different fractionation techniques have been utilized (centrifugation, filtration, FFF) in combination with ICP-MS in an attempt to examine only the size fraction of nanomaterials under consideration. However this approach can introduce artifacts that may significantly alter the original state of the material.

This promising development in spICP-MS could allow for the simultaneous detection of multiple elements, which can then be used to discriminate between naturally occurring nanomaterials and ENPs. Nanomaterials found in the environment generally consist of a chemically complex elemental make-up, when contrasted to the elementally pure ENPs¹⁴. One such example is cerium and lanthanum which occurs in the environment in a ratio of 1.70 ± 0.54 as reported for 807 samples found in the Geochemical Atlas of Europe.⁴⁴ By contrast, an engineered cerium oxide nanoparticle would likely be enriched in cerium. Utilizing the dual-element capability of micro-second dwell time spICP-MS, the detection of engineered ceria nanoparticles would be realized by particle containing only cerium, as opposed to naturally occurring analogues containing a fixed ratio of cerium and lanthanum as shown in figure 7. Here two samples were analysed using dual-element spICP-MS with 100

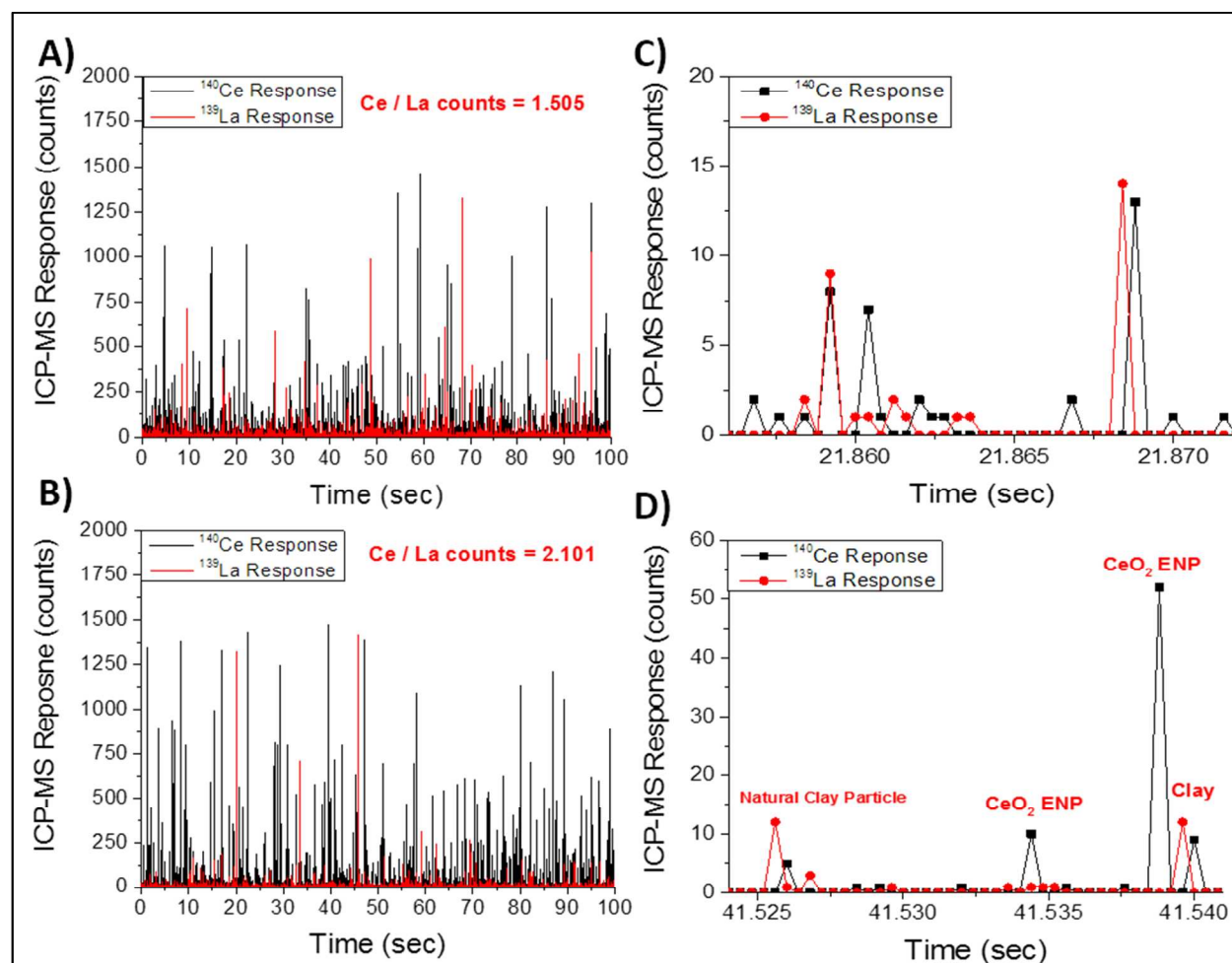


Fig. 7. Analysis of Clear Creek stream water using dual element microsecond spICP-MS. a) Raw data of Clear Creek stream water. b) Raw data of Clear Creek stream water with 80-100 nm spiked CeO₂ ENPs. c) Magnified section of figure 7a showing presence of particles containing both cerium and lanthanum. d) Magnified section of figure 7b showing presence of particles containing cerium and lanthanum as well as only cerium, which may indicate the presence of engineered CeO₂.

μ s dwell time and a 100 μ s settling time. A sample of stream water collected from Clear Creek in Golden, Colorado, U.S.A was monitored for both ¹³⁹La and ¹⁴⁰Ce (fig 7a and 7c). In figure 7b and 7d, cerium dioxide nanoparticles (80-100 nm) were spiked into the stream water, shifting the ratio of cerium to lanthanum counts towards higher cerium content. This is further demonstrated by the presence of cerium only peaks shown in figure 7d. A limiting factor will be the difference in masses between the two elements being analysed, as this will determine the shortest settling time achievable by the instrument. In addition, both elements will need to be present in appreciable amounts to be detected, as the absence of the “natural” element may result in false positives of ENP detection. Despite these limitations, this proposed method may be able to extend to different naturally occurring nanoparticles and emerging ENPs. Further development of microsecond spICP-MS may allow researchers to exploit this approach for environmental fate studies of ENPs.

Materials and Methods.

Reagents

To generate Au and Ag calibration curves of known mass concentrations, a set of dissolved analyte standards was used. For the dissolved silver standards, a stock solution of silver nitrate (Perkin Elmer Pure, atomic spectroscopy standard) was diluted using 2% optima grade nitric acid (Fisher Scientific) to concentrations from 0 to 500 ppb. Dissolved gold standards (Spex CertiPrep, spectroscopy standard) were made through the dilution of a stock solution of gold chloride using 2% optima grade hydrochloric acid (Fisher Scientific) to concentrations of 0 to 10 ppb. Gold nanoparticles (100 nm) capped with a citrate stabilizer to prevent aggregation were purchased from BBI Solutions and used to determine transport efficiency. Citrate-capped 60 and 100 nm silver nanoparticles were purchased from NanoComposix, Inc. Au/Ag particles were custom synthesized with a 30 nm gold core and 30 nm silver shell for a total diameter of 60 nm as purchased from NanoComposix, Inc. Cerium oxide (CeO₂) nanoparticles with diameters between 50-80nm were purchased from Inframat® Advanced Materials™ as a solid power and were suspended in water via sonication. All nanoparticle solutions were prepared by dilution of the stock solution using ultrapure deionized water, 18.2 mΩ resistivity, from a Barnstead International Nanopure Diamond™ purification system. Clear Creek stream water was

collected in 250 mL polypropylene containers and diluted prior to analysis by spICP-MS.

Instrumentation

A quadrupole ICP-MS (Nexion 300Q, Perkin Elmer), equipped with a Type-C Miramist nebulizer and baffled cyclonic spray chamber, was operated using instrumental conditions described in SI. Software developed for this project provided for both data collection at microsecond dwell times and, for single element measurements, the elimination of the quadrupole settling time between readings. The analysis of gold core-silver shell nanoparticles (Au/Ag NPs) was performed using a 100 microsecond dwell time and 100 microsecond settling time for each mass. The settling time was used to account for ion flight time through the quadrupole mass analyzer and to the detector. This was initially calculated based on the most probable ion kinetic energies for gold and silver ions and later verified in-lab using gold and silver standard aqueous solutions. Settling times shorter than 100 microseconds caused a discernable drop in Au and Ag signal intensities, indicating that the mass analyzer electronics are potentially switching faster than the ions are able to clear the mass analyzer. As a result, 100 microseconds was chosen as a suitable settling time. To further validate the composition of the Au/Ag NPs sedimentation field-flow fractionation (CF2000 PostNova Analytics) and asymmetrical flow-field flow fractionation-ICP-MS (AF4-2000 PostNova Analytics) were coupled to the NexION 300Q. (SI figure 5).

Nebulizer Transport Efficiency

An important aspect of single particle ICP-MS analysis is the determination of the nebulizer transport efficiency. This term represents the fraction of aqueous sample that reaches the plasma. A mass-based nebulization efficiency was determined for the work presented here. For this method, a standard particle (i.e. gold) of known size is used and its count intensity is compared to that of a series of dissolved gold standards to determine the transport efficiency.^{25, 45} This transport efficiency is then applied to the remaining analytes of interest, Ag in this study, to develop an accurate mass-flux calibration curve which is used in converting the counts generated by a nanoparticle into a mass.

A more straightforward method is to compare the measured pulse number frequency of a known particle standard to the expected particle number concentration, as the ratio of these two values being the transport efficiency. The absence of a particle number standard in the commercial market, and potential NP losses during sample storage, diminishes the feasibility of this method. The software reported here allows for the determination of nebulization efficiency by either a mass-based method or a number-based method. In addition, multiple standard particle sizes can be used to create a particle size calibration curve.

Tuoriniemi et al. discuss different alternative methods to determine transport efficiency by taking into account the sample flow rate, waste flow rate and the respective analyte signals in both the sample and waste fractions.⁴⁵ Another means of improving nebulization efficiency is to utilize micro-droplet generators which can produce micro-droplets of a fixed diameter containing the analyte.³⁷ By accelerating the desolvation of the micro-droplets through the use a lighter carrier gas such as helium, nebulization efficiencies can

improve to as high as 100%.³⁸ This technique however requires extra instrumentation beyond the typical nebulizer setups commonly found for most ICP-MS configurations.

Data Collection and Processing

A commercially available software package, Syngistix™ Nano Application Module, designed for NexION ICP-MS by Perkin Elmer was used throughout the experiments for data acquisition and further processing of the raw intensity data to particle size distribution information, as shown SI figures 6 and 7. The software package enables the instrument to acquire transient data continuously with short dwell times (e.g. 0.1 ms used for this work). Background count threshold in the raw data is determined real-time using a method which employs an average plus 3σ described previously (Pace et al.) and nanoparticle events are detected based on the calculated background threshold.³⁴ Peak area for each nanoparticle event is determined by summing the data points that construct the event. The peak area information is then converted to particle size assuming spherical particle shape and based on calibration curves constructed from solution or nanoparticle standards.

Conclusions

At a time where there is a great need for sophisticated instrumentation and more sensitive analytical techniques, spICP-MS has proven to be a powerful tool for the detection and characterization of ENPs in environmental samples. By utilizing microsecond dwell times, the resolution and working range of this technique has been improved to analyze an even greater breadth of environmental samples and increasingly complex matrices. Obstacles arising from relatively high particle number concentrations and high backgrounds of dissolved analyte can be overcome to provide a more accurate representation of the number and size of engineered nanoparticles in solution. Moreover, the addition of dual-element detection capability could prove instrumental in distinguishing naturally occurring particle from their engineered counter-parts without significant sample preparation. The simultaneous development of the Nano software not only makes microsecond spICP-MS possible, it puts this tool into the hands of analysts who which to add spICPMS capabilities to their laboratory.

Though the microsecond technique helps overcome a number of obstacles of conventional millisecond spICP-MS, it does have a number of obstacles. Some data at the edges of the pulse may be lost to the background signal, and thus be excluded from the overall intensity of the particle. Additionally, since the dwell time is reduced, the count intensity generated by the nanoparticle is parsed into 2-4 reading according to the dwell time window. Consequently, the spacing between sampling events decreases, the intensity within the sampling event will also decrease. As a result, even though resolution between particle events increases, the overall detection limit with respect to size increases.

Work remains to be done to further develop this technique and improve its sensitivity, but in its current state, it is a premiere technique for engineered nanomaterial detection and characterization.

Acknowledgements

This body of work was supported by the Semiconductor Research Corporation (CSM Task Order 425.040)

The authors would like to thank Pritesh Patel and Dylan MacNair (Perkin Elmer, Inc.) for their development of the software necessary for the analysis of nanoparticles at microsecond dwell times.

Soheyl Tadjiki (PostNova Analytics) for his instruction and assistance in acquiring sedimentation-FFF fractograms of the gold-silver nanocomposites.

In addition, the authors would thank Gary Zito and John Chandler (Colorado School of Mines) for their assistance in obtaining images of the gold-silver nanocomposites by scanning electron microscopy. Chris Higgins provided valuable discussions on the spICPMS method development.

Notes and references

^a Colorado School of Mines, Dept. of Chemistry and Geochemistry, Golden, CO 80401, United States of America

^b PerkinElmer, Inc., Woodbridge, Ontario, L4L 8H1, Canada

Electronic Supplementary Information (ESI) available: [Table of typical NexION 300Q operating conditions, TEM images of particles used in this study with accompanying EDX spectra, additional plots of improvements in coincidence and reduction in dissolved background signals, screen captures of commercial software in use for the analysis of nanoparticles.]. See DOI: 10.1039/b000000x/

- M. E. Leitch, E. Casman and G. V. Lowry, *Journal of Nanoparticle Research*, 2012, **14**, 1-23.
- G. C. Delgado, *Technology in Society*, 2010, **32**, 137-144.
- A. Nel, T. Xia, L. Mädler and N. Li, *Science*, 2006, **311**, 622-627.
- S. Gavankar, S. Suh and A. Keller, *The International Journal of Life Cycle Assessment*, 2012, **17**, 295-303.
- S. J. Klaine, P. J. J. Alvarez, G. E. Batley, T. F. Fernandes, R. D. Handy, D. Y. Lyon, S. Mahendra, M. J. McLaughlin and J. R. Lead, *Environmental Toxicology and Chemistry*, 2008, **27**, 1825-1851.
- B. Nowack, J. F. Ranville, S. Diamond, J. A. Gallego-Urrea, C. Metcalfe, J. Rose, N. Horne, A. A. Koelmans and S. J. Klaine, *Environmental Toxicology and Chemistry*, 2012, **31**, 50-59.
- P. Westerhoff and B. Nowack, *Accounts of chemical research*, 2012, **46**, 844-853.
- A. Nel, T. Xia, H. Meng, X. Wang, S. Lin, Z. Ji and H. Zhang, *Accounts of chemical research*, 2012, **46**, 607-621.
- F. Gottschalk, T. Sonderer, R. W. Scholz and B. Nowack, *Environmental Science & Technology*, 2009, **43**, 9216-9222.
- N. C. Mueller and B. Nowack, *Environmental Science & Technology*, 2008, **42**, 4447-4453.
- B. Nowack, H. F. Krug and M. Height, *Environmental Science & Technology*, 2011, **45**, 1177-1183.
- C. Beaudrie and M. Kandlikar, *Journal of Nanoparticle Research*, 2011, **13**, 1477-1488.
- C. E. H. Beaudrie, M. Kandlikar and T. Satterfield, *Environmental Science & Technology*, 2013, **47**, 5524-5534.
- F. von der Kammer, P. L. Ferguson, P. A. Holden, A. Masion, K. R. Rogers, S. J. Klaine, A. A. Koelmans, N. Horne and J. M. Unrine, *Environmental Toxicology and Chemistry*, 2012, **31**, 32-49.
- P. J. J. Alvarez, V. Colvin, J. Lead and V. Stone, *ACS Nano*, 2009, **3**, 1616-1619.
- M. Hasselov, J. Readman, J. Ranville and K. Tiede, *Ecotoxicology*, 2008, **17**, 344-361.
- M. S. Jiménez, M. T. Gómez, E. Bolea, F. Laborda and J. Castillo, *International Journal of Mass Spectrometry*, 2011, **307**, 99-104.
- F. Laborda, J. Jimenez-Lamana, E. Bolea and J. R. Castillo, *Journal of Analytical Atomic Spectrometry*, 2011, **26**.
- H. Kawaguchi, N. Fukasawa and A. Mizuike, *Spectrochimica Acta Part B: Atomic Spectroscopy*, 1986, **41**, 1277-1286.
- C. Degueldre and P.-Y. Favarger, *Colloids and Surfaces A: Physicochemical and Engineering Aspects*, 2003, **217**, 137-142.
- C. Degueldre and P.-Y. Favarger, *Talanta*, 2004, **62**, 1051-1054.
- C. Degueldre, P. Y. Favarger and C. Bitea, *Analytica Chimica Acta*, 2004, **518**, 137-142.
- C. Degueldre, P.-Y. Favarger, R. Rosse and S. Wold, *Talanta*, 2006, **68**, 623-628.
- C. Degueldre, P.-Y. Favarger and S. Wold, *Analytica chimica acta*, 2006, **555**, 263-268.
- H. E. Pace, N. J. Rogers, C. Jarolimek, V. A. Coleman, C. P. Higgins and J. F. Ranville, *Analytical Chemistry*, 2011, **83**, 9361-9369.
- J. Tuoriniemi, G. Cornelis and M. Hasselöv, *Analytical Chemistry*, 2012, **84**, 3965-3972.
- J. G. Coleman, A. J. Kennedy, A. J. Bednar, J. F. Ranville, J. G. Laird, A. R. Harmon, C. A. Hayes, E. P. Gray, C. P. Higgins and G. Lotufo, *Environmental Toxicology and Chemistry*, 2013, **32**, 2069-2077.
- L. D. Scanlan, R. B. Reed, A. V. Loguinov, P. Antczak, A. Tagmount, S. Aloni, D. T. Nowinski, P. Luong, C. Tran, N. Karunaratne, D. Pham, X. X. Lin, F. Falciani, C. P. Higgins, J. F. Ranville, C. D. Vulpe and B. Gilbert, *ACS Nano*, 2013.
- R. B. Reed, D. G. Goodwin, K. L. Marsh, S. S. Capracotta, C. P. Higgins, D. H. Fairbrother and J. F. Ranville, *Environmental Science: Processes & Impacts*, 2013, **15**, 204-213.
- D. M. Mitrano, E. K. Leshner, A. Bednar, J. Monserud, C. P. Higgins and J. F. Ranville, *Environmental Toxicology and Chemistry*, 2012, **31**, 115-121.
- E. P. Gray, J. G. Coleman, A. J. Bednar, A. J. Kennedy, J. F. Ranville and C. P. Higgins, *Environmental Science & Technology*, 2013.
- K. Loeschner, J. Navratilova, C. Koblner, K. Mølhave, S. Wagner, F. Kammer and E. Larsen, *Analytical and Bioanalytical Chemistry*, 2013, **405**, 8185-8195.
- R. B. Peters, Z. Rivera, G. Bommel, H. P. Marvin, S. Weigel and H. Bouwmeester, *Analytical and Bioanalytical Chemistry*, 2014, 1-11.
- H. E. Pace, N. J. Rogers, C. Jarolimek, V. A. Coleman, E. P. Gray, C. P. Higgins and J. F. Ranville, *Environmental Science & Technology*, 2012.
- J. Liu, K. E. Murphy, R. I. MacCuspie and M. R. Winchester, *Analytical chemistry*, 2014.
- J. W. Olesik and P. J. Gray, *Journal of Analytical Atomic Spectrometry*, 2012, **27**, 1143-1155.
- S. Gschwind, L. Flamigni, J. Koch, O. Borovinskaya, S. Groh, K. Niemax and D. Gunther, *Journal of Analytical Atomic Spectrometry*, 2011, **26**, 1166-1174.
- J. Koch, L. Flamigni, S. Gschwind, S. Allner, H. Longrich and D. Gunther, *Journal of Analytical Atomic Spectrometry*, 2013, **28**, 1707-1717.
- G. Cornelis and M. Hasselov, *Journal of Analytical Atomic Spectrometry*, 2014, **29**, 134-144.
- O. Borovinskaya, B. Hattendorf, M. Tanner, S. Gschwind and D. Günther, *Journal of Analytical Atomic Spectrometry*, 2013, **28**, 226-233.
- F. Laborda, J. Jimenez-Lamana, E. Bolea and J. R. Castillo, *Journal of Analytical Atomic Spectrometry*, 2013, **28**, 1220-1232.
- O. Borovinskaya, B. Hattendorf, M. Tanner, S. Gschwind and D. Gunther, *Journal of Analytical Atomic Spectrometry*, 2013, **28**, 226-233.
- J. R. White and A. E. Cameron, *Physical Review*, 1948, **74**, 991-1000.
- R. Salminen, 2005.
- J. Tuoriniemi, G. Cornelis and M. Hasselov, *Journal of Analytical Atomic Spectrometry*, 2014.

